



## BLOOD VESSELS SEGMENTATION BASED ON THREE RETINAL IMAGES DATASETS

Sara Bilal<sup>1</sup>, Fatin Munir<sup>2</sup> and Mostafa Karbasi<sup>3</sup>

<sup>1</sup>Department of Science, International Islamic University Malaysia, Malaysia

<sup>2</sup>Department of Electrical Engineering, Kuliyah of Engineering, International Islamic University Malaysia

<sup>3</sup>Department of Computer Science, Kuliyah of Information and Communication Technology, International Islamic University Malaysia, Malaysia

E-Mail: [sarra@iiu.edu.my](mailto:sarra@iiu.edu.my)

### ABSTRACT

Retinal images are routinely acquired and retinal blood vessels are segmented to provide diagnostic evidence of diabetic retinopathy. Due to the acquisition process, usually these images are non-uniformly illuminated and demonstrate local luminosity and contrast variability. Based on four image processing techniques, namely, Matched filter, Hough transform, Morphological operations and Watershed, the retinal blood vessels have been segmented. Then, their strengths and weaknesses are mathematically compared in terms of retinal images segmentation. Each algorithm performance was tested on DRIVE, DRIONS and High-Resolution Fundus images database. The results show that measuring the automatic segmentation algorithm performance is based mainly on how the retinal images are acquired as well as the image processing technique used for segmentation. Neural Network has been used to recognize the retinal images. The obtained results could help the eye specialists to visually examine the retinal images.

**Keywords:** retinal images, eye blood vessels, segmentation, database, neural network.

### INTRODUCTION

Ophthalmologist can detect and diagnosis many eye diseases that can cause blindness like glaucoma and diabetic retinopathy in time only by the help of retinal images. Diabetes is a severe health problem especially in developed countries, with estimated numbers about 366 million diabetes cases globally in 2030. The difference between retinal image for normal and diabetic person is shown in Figure-1.

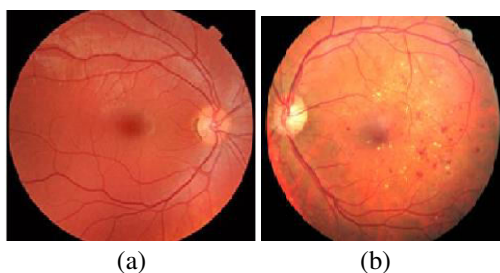


**Figure-1.** (a) Retinal image for normal person (b) Retinal image for diabetic person [2].

Therefore, automatic detection of blood vessels is very important because it can help to detect the early symptoms of diabetic automatically rather than using the conventional blood test for diagnosing diabetic in hospitals. Automatic detection can determine any pathological changes in the length, width, tortuosity and branching pattern of the blood vessels as well as grade of severity of disease or automatically diagnosis the diseases. Manual detection is so difficult because:

1. A number of images are required to judge of a disease in the retinal images.

2. Complexity and low contrast of the blood vessels in the retinal images. So automatic methods are required for detecting and measuring the vessels in retinal image.

In spite of developing of many approaches for detecting and extracting retinal images, there is lack, eg. in the segmentation accuracy results.

### Research background

Several methods are available to segment the retinal images (see Figure-2) among which one can name Matched filter, Hough transform, edge detection, Morphological operations and watershed.

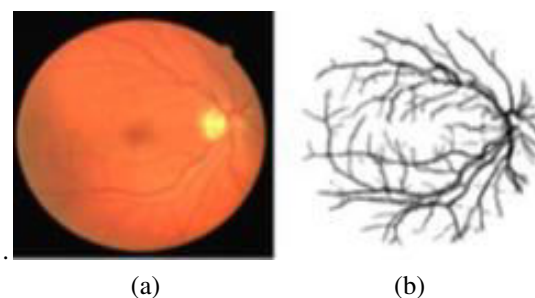


**Figure-2.** Examples of retinal images and its segmentation results [3].

### A. Matched Filter (MF)

Matched filter (MF) is a template matching the algorithms implemented in the detection of retinal images



blood vessels [4]. The piecewise linear segments can be detected in retinal images blood vessels. Basically in MF, a two-dimensional linear has a Gaussian cross-profile section which can be rotated into three dimensions. Then, the cross-profile of the retinal blood vessel can be identified by that rotation, which typically enjoys a Gaussian or a Gaussian derivative profile as shown in Figure-3. Many different orientations (usually eight or 12) are rotated to the kernel to fit into the retinal blood vessels of different configurations.

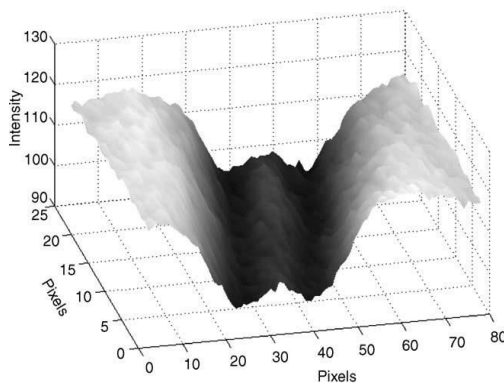


**Figure-3.** An intensity profile from three-dimensional image of "double-Gaussian" construct in retinal blood vessel [5].

Then, by the use of thresholding of retinal images, the blood vessels from background can be differentiated.

All the features are divided by an arbitrary chosen gray level into binary classification, but according to their intensity level towards brightness threshold [6]. By anyway, this is applicable on healthy retinal images only, (e.g) in diabetic retinopathy it's difficult to detect very fine neovascularization due to change in image resolution in

- (1) Background intensity
- (2) Reduced contrast to noise ratio.

Non linear "tram-line" filter can solve the problem by the use of contrast between a central line oriented along the retinal blood vessels and satellite tram-line at either side [7]. But its disadvantages are that it might be tough to fit into highly tortuous vessels if we use of the longer structuring element.

Figure-4 shows an original retinal image and its gray-level profile of some cross section [1].

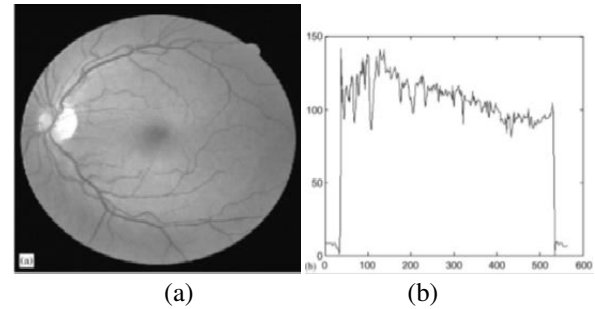


**Figure-4.** (a) The green band of a digital retina image (b) Profile of a one pixel width at the 200th row of the retina image [1].

MF according to properties of blood vessels can be designed as follows:

- (a) Vessels can be calculated as anti parallel segments.
- (b) The vessel look relatively darker than background because they have lower reflectance compare to other retinal surface.
- (c) Vessel size may reduce & width of a retina vessel may lie within the range of 2-10 pixels when it is going far away from optic disc.
- (d) Intensity profile will changed slightly from vessel to vessel.
- (e) The intensity profile has a Gaussian shape.

## B. Hough Transform (HT)

In computer image processing, HT is an algorithm which is usually used to detect geometry of objects. Through this method some points lying within the lines, circles and other curves will be easily detected in an image.

$n$  points in an image are (typically a binary image), supposedly used to find subsets of the points that lying on straight lines. A probable way is to initially find all lines determined by each pair of points and then find all subsets of points near the particular lines [8]

On the other hand, with the HT, considered that a point  $(x_i, y_i)$  and all the lines that pass through it. Infinite number of lines pass through  $(x_i, y_i)$ , all of which satisfy the slope-intercept line equation  $y_i = ax_i + b$  for some values of  $a$  and  $b$ . Writing the equation as  $b = -x_i a + y_i$  and taking the  $ab$ -plane (parameter space) into account gives the equation of a single line for a fixed pair  $(x_i, y_i)$ . Besides, a second point  $(x_j, y_j)$  has an associate line in parameter space which intersects its associated line  $(x_i, y_i)$  at  $(a', b')$  in which  $a'$  is the slope and  $b'$  the intersect of the line containing both  $(x_i, y_i)$  and  $(x_j, y_j)$  in the  $xy$  plane. Actually, all points on this line have lines in parameter space intersecting at  $(a', b)$ . Figure-6 demonstrates the concept.

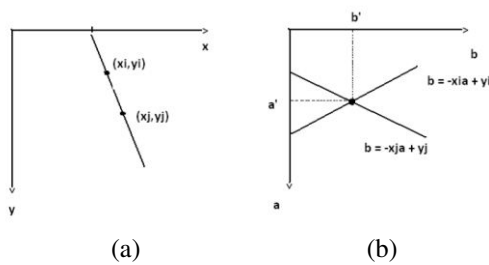


Figure-5. (a)  $xy$  plane (b) Parameter space [8].

Basically, the parameter-space lines corresponding to all image points  $(x_k, y_k)$  in the  $xy$ -plane could be plotted, and the principal lines in that plane could be found by identifying points in parameter space where large number of parameter-space lines intersect. However, a problem is that as the line slope approaches infinity as the line approaches the vertical direction. An approach to deal with this stumbling block is to use the normal representation of a line:

$$x \cos \theta + y \sin \theta = \rho \quad (1)$$

where

$\rho$  = the line distance from the origin

$\theta$  = the angle between the perpendicular and the  $x$ -axis.

The optic disc in colour retinal images was identified and modelled by Rotaru et al in 2014 [9].

The optic disc in two steps are localised. By first three approaches: (a) the optic disc area is detected on texture indicate and pixel intensity variance analysis in the green component of RGB image. (b) on the segmented area, the optic disc edges are extracted and the resulted boundary is approximated by a Hough transform. The last implemented method identifies the optic disc area by analysing blood vessels network extracted in the green channel of the original image. To obtain the optic disc edges in the segmented area, an iterative Canny algorithm is used. The edges are then approximated by a circle Hough transforms.

### C. Morphological operations

To analyse shapes in images, mathematical morphology in image processing is quite appropriate. Two main processes are dilation and erosion which involve a special mechanism of combining two sets of pixels. Usually, one set includes the image under process and the other is a smaller set of pixels known as a structuring element or kernel. Throughout this section, a default kernel of size  $3 \times 3$  is used. Morphological operations can also be applied to gray-level images to reduce noise or brighten the image.

### D. Watershed

The watershed segmentation can be described by setting  $M_1, M_2, \dots, M_r$  which denote the minimum area of the retinal image to be segmented.  $C(M_i)$  denotes basin which is related to the minimum area  $M_i$ , min and max denote the minimum value and maximum value of the gradient. The overflow process is carried out by a single gray scale value increase. Then we set  $n$  denotes the increases of overflow value (the depth of overflow in step  $n$ ),  $T[n]$  represents the set of all points meeting  $f(x) < n$ , and  $f(x)$  is signal of the gradient image. For a given basin, the overflow may occur at different degrees in step  $n$  (or may not). Suppose a minimum area  $M_i$  overflows in step  $n$ , and  $C_n(M_i)$  is part of basin related to  $M_i$ , that is the area consisted of horizontal plane formed in basin  $C(M_i)$ . The binary image  $C_n(M_i)$  can be expressed as :

$$C_n(M_i) = C(M_i) \cap T[n] \quad (2)$$

If the gray scale value of the minimum area  $M_i$  is  $n$ , then in step  $n+1$ , the overflow of basin and minimum area will be exactly the same, that is,  $C_{n+1}(M_i) = M_i$ . Set  $C[n]$  denotes the union of basin overflow in step  $n$ , then  $C[\max+1]$  is the union of all the basins, and the algorithm is initialized with  $C[\min+1] = T[\min+1]$ .

The overflow is defined recursively, so if  $C[n-1]$  has been established, according to the formula (3.7),  $C[n]$  is a subset of  $T[n]$ . Also we know that  $C[n-1]$  is a subset of  $C[n]$ , so  $C[n-1]$  is a subset of  $T[n]$ , and then there will be three situations:

$D \cap C[n-1]$  is empty;

$D \cap C[n-1]$  is non-empty, and containing one connected component of  $C[n-1]$ ;

$D \cap C[n-1]$  is non-empty, and containing multiple connected component of  $C[n-1]$ .

Situation (1) will occur when the growing overflow reaches a minimum area. For situation (2),  $D$  locate in some minimum area. For situation (3), some basins  $C_{n-1}(M_i)$  consisted in  $C[n-1]$  must be contained in  $D$ .

### EXPERIMENTAL RESULTS

As shown in Figure-7, retinal blood vessels segmentation process and recognition can be divided into three stages.

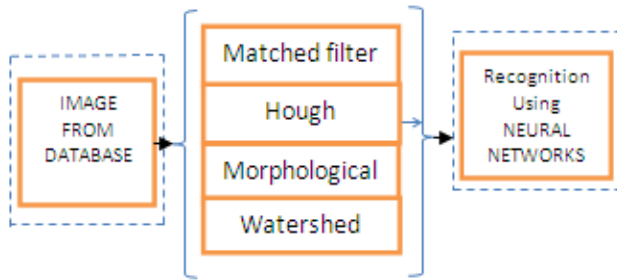


**Figure-6.** Retinal image blood vessels segmentation and recognition.

### A. Image from Database

For research purposes there are several retinal databases. However, because of their availability and popularity, here three types of retinal image databases, namely, DRIVE, Drions and High-Resolution Fundus (HRF) are used.

#### Drive Database

DRIVE database includes retinal images which are JPEG compressed. Each image was captured using 8 bits per colour plane at 768 by 584 pixels. As shown in Figure-8, this database contains 40 images, 20 for training and 20 for testing.

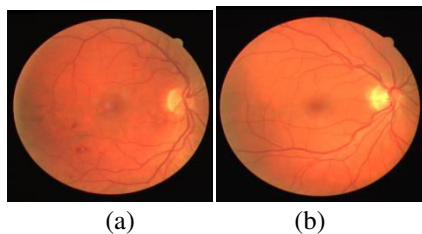


**Figure-7.** Retinal images from DRIVE databases (a) Healthy retinal images (b) Diabetic Retinopathy image.

#### Drions Database

The segmentation of the optic nerve head dealing for creating data base. It contains 110 images with 2 ground truths for each one which has two medical expert. Images were digitized using a HP-PhotoSmart-S20 high-resolution scanner, RGB format, resolution 600x400 and 8 bits/pixel as shown in Figure-9.

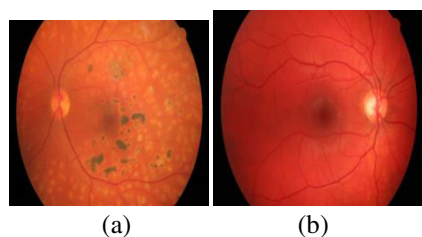


**Figure-8.** Retinal Images from DRIONS database (a) Healthy retinal image (b) Diabetic retinopathy image.

### High Resolution Fundus (HRF) Database

Three set of different categories such as fundus, healthy and pathological eyes contain in the database. A section of database contains gold standard images of manually segmented blood vessels. The first set is composed of 15 images of healthy patient with no retinal pathology. The second categories include 15 retinal images of patients with DR and the last set includes 15 images of patients with advanced stage glaucoma. The size of image is  $3504 \times 2336$  pixels as shown in Figure-10.

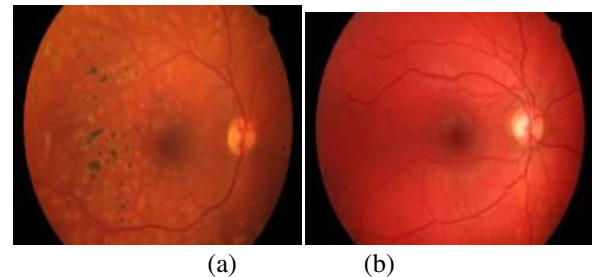


**Figure-9.** Retinal Images from DRIONS database (a) Healthy retinal image (b) Diabetic retinopathy image.

### B. Retinal images blood vessels segmentation

The proposed segmentation of retinal blood vessels will be implemented through three methods: Matched filtering, Hough transform and Morphological operations.

#### i. Matched Filter (MF)

The Matched filter kernel can be obtained by using the following equation:

$$K_i(x, y) = -e^{-x^2/2\sigma^2}, \text{ for } |y| \leq L/2 \quad (3)$$

Length of vessel is shown by  $L$  with fix orientation. It is assumed that the y-axis is aligned with direction of vessel.

The value of the  $x$  varies from  $-3\sigma$  to  $+3\sigma$ . This kernel is rotated in  $15^\circ$  steps, generating 12 filters. For each filter, the mean is obtained:

$$M_i = \sum P_i \in N \frac{K_i(x, y)}{A} \quad (4)$$

Number of elements of kernels denoted by  $A$  and kernel  $i$  point is shown with  $P_i$ , the final kernel is shown by

$$K_i' = (x, y) = K_i(x, y) - m_i \quad (5)$$

For an image applied set of 12 such filters and retained only maximum value of all filters for each pixel.





## ii. Retinal images segmentation using matched filter

Figure-11 shows retinal images which consist of diabetes retinopathy for three types of databases which are Drives, Drions and HRF. Figure-12 shows the segmented results of the three database sets using Matched filter.

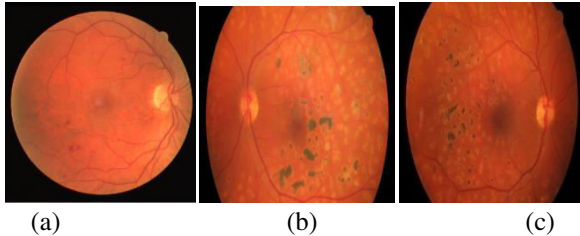


**Figure-10.** (a) Drive Database (b) Drions Database (c) HRF Database.

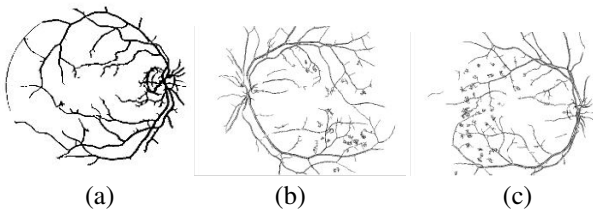


**Figure-11.** Segmented images using Matched filter (a) Drive database (b) Drions Database (c) HRF Database.

It is clear that the diabetic cells in Drions and HRF databases in Figure-12 (b) and (c) have been segmented successfully. Meanwhile, the optic fovea centre in image of DRIVE has better segmentation using Matched filter as shown in Figure 12 (a) comparable to the results obtained from Drions and HRF databases.

## iii. Hough Transform (HT)

The conventional HT can be commonly used for detection of regular curves such as lines, circles and ellipses. If a line exists in the image, it will be in accordance with a polar equation given by

$$\rho = m \cos \theta + n \sin \theta \quad (6)$$

Where  $\rho$  = the length of a normal vector from the origin  
 $\theta$  = the orientation of  $\rho$  with respect to the x-axis.  $r$  and  $\theta$  are constant for any point  $(m, n)$  in this line.

## b. Retinal images segmentation using hough transform

Figure-13 shows retinal images which consist of diabetes retinopathy for three types of databases which are Drives, Drions and HRF. Figure-14 shows the segmented results of the three database sets using Hough Transform, respectively.

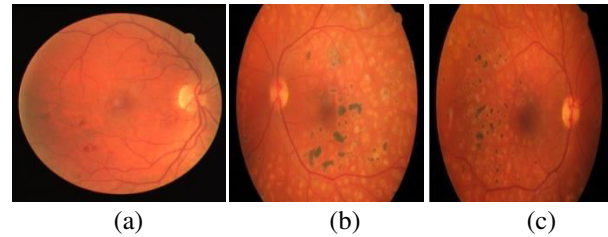


**Figure-12.** (a) DRIVE database (b) Drions database (c) HRF database.

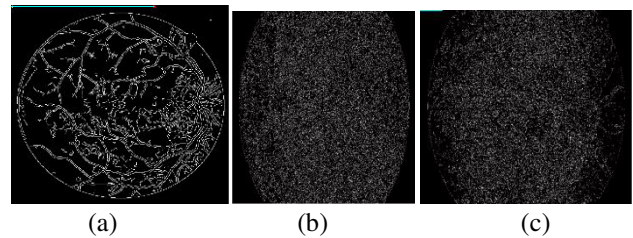


**Figure-13.** Segmented retinal images using Hough transform (a) DRIVE database (b) Drions database (c) HRF database.

From the results above, it is clear that DRIVE database has a better segmented retinal image using Hough transform as shown in Figure-14 (a). Meanwhile, the segmentation results as shown in Figure-14 (b) and (c) for Drions and HRF, respectively, was not successful using Hough transform. For optic fovea, all the retinal images from three types of databases do not have better segmentation using Hough transform as shown in Figure-14 (a), (b) and (c).

## c. Retinal images segmentation using morphological operations

Dilation and erosion are the Morphological operations which have been used in this work on a grayscale image.

Figure-14 shows retinal images which consist of diabetes retinopathy for three types of databases which are DRIVES, Drions and HRF. Figure-15 shows the segmented results of the three database sets using Morphological operations.

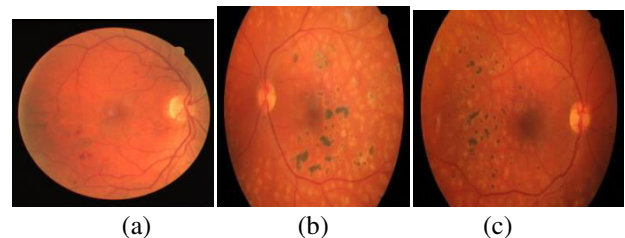


**Figure-14.** (a) DRIVE database (b) Drions database (c) HRF database.

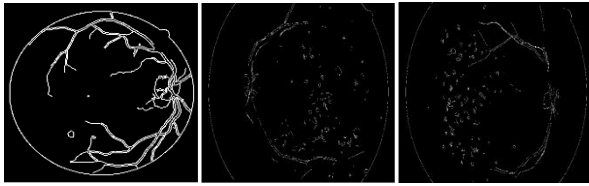


**Figure-15.** Segmented retinal images using Morphological  
(a) DRIVE database (b) Drions database (c) HRF database.

From the results, it is clear that the diabetic retinopathy has been successfully segmented as shown in Figure-15(a), (b) and (c). However, using this method, the segmentation in retinal image using DRIVE database is more accurate (see Figure 16 (a)) compared with Drions and HRF databases as shown in Figure-15 (b) and (c). As well, for optic fovea, DRIVE database in Figure-15 (a) has better segmentation as shown comparable to the results obtained from Drions and HRF databases.

#### d. Retinal image segmentation using watershed

Figure-17 shows retinal images which consist of diabetes retinopathy for three types of databases which are Drive, Drions and HRF. Meanwhile for Figure-18, it is illustrates the segmented results of the three databases sets using watershed.

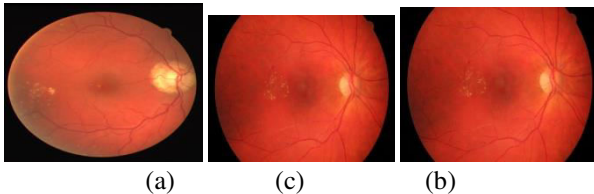


**Figure-17.** (a) Drive database (b) Drions database (c) HRF database.

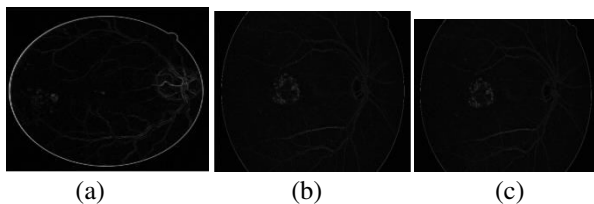


**Figure-18.** Segmented retinal images using watershed (a) Drive database (b) Drions database (c) HRF database.

From the results above, it is clear that the diabetic cells in Drive, Drions and HRF datasets in Figure-17 (a), (b) and (c) have been segmented based on Figure-18 (a), (b) and (c) respectively.

For optic fovea, Drive database in Figure 18 (a) has better segmentation as shown comparable to the results from Drions and HRF database.

#### MEASURE OF BLOOD VESSELS SEGMENTATION ACCURACY

The effectiveness of the automatic segmentation methods was measured by the following parameters:

1-Percentage of non-vessel pixels classified as vessel pixel shown as False Positive (FP)

2- Harmonic mean of Precision (P) and Recall(R) shown by F-measure. Where, the best value for F-measure is at 1 and worse score at 0. [10]

$$R = \frac{TP}{TP+FN} \quad (7)$$

$$P = \frac{TN}{TN+FP} \quad (8)$$

$$F\text{-measure} = (2 * P * R) / (P + R) \quad (9)$$

where  $TP$  = True Positive

$FN$  = False Negative

Tables 1, 2 and 3 show the aforementioned segmentation measurements based on the three databases which are Drive, Drions and HRF, respectively.

**Table-1.** Segmentation accuracy measurements using matched filter.

Measurements	$TP$	$FP$	$F$ measure
<i>Drive</i>	0.95	0.043	0.954
<i>Drions</i>	0.96	0.06	0.94
<i>HRF</i>	0.96	0.069	0.95

**Table-2.** Segmentation accuracy measurements using hough transform.

Measurements	$TP$	$FP$	$F$ measure
<i>Drive</i>	0.0013	0.00025	0.0026
<i>Drions</i>	0.0013	0.016	0.00026
<i>HRF</i>	0.00035	0.0166	0.00069

**Table-3.** Segmentation accuracy measurements using morphological operation.

Measurements	$TP$	$FP$	$F$ measure
<i>Drive</i>	0.025	0.019	0.047
<i>Drions</i>	0.0035	0.0166	0.007
<i>HRF</i>	0.0035	0.0165	0.007

**Table-4.** Segmentation accuracy measurements using watershed.

Measurements	<i>TP</i>	<i>FP</i>	<i>F</i> measure
<i>Drive</i>	0.025	0.019	0.047
<i>Drions</i>	0.0035	0.0166	0.007
<i>HRF</i>	0.0035	0.0165	0.007

**Recognition using neural network**

For recognition, ANN named Multi-layer Feed-forward Neural Network (MLFNN) with Back-Propagation (BP) algorithm is applied. This ANN works by sending the signals forward while the errors will be propagated backwards. The idea of this algorithm is to reduce the error which is the difference between actual and expected results. Besides that, it is used to provide more suitable weight for the network so that all input can results in the output targeted. The back-propagation learning algorithm with single hidden layer of MLFNN has been used. The input layer consists of 7 nodes and different numbers of hidden layer are used to compare which one gives a good result. The number of hidden layer are used in this research are 5, 10 and 15. There is only a single output of this network which gives the real-valued output between 0 and 1. The activation function used is the log sigmoid for both hidden and output layer. The initial weights were chosen randomly and each retinal image from three types of database has been segmented using four algorithms which then been fed into the network for training phase. There are 30 retinal images in each database, 18 retinal images are used for the training, and another 12 retinal images have been used for the validation and testing phase. In order to get accurate results, the network has been trained five times due to limited retinal images in each database which are 30. The results of testing confusion matrix and the number of epoch in each database and segmentation have been recorded which then are compared with each other. From the results of testing confusion matrix, we can know the retinal images that have been recognized successfully by the trained system. Tables 4, 5 and 6 show the overall percentage rate of testing confusion matrix in each database and segmentation with three different nodes in hidden layer.

**1. Hidden layer = 5 nodes****Table-5.** Overall percentage rate of testing confusion matrix in each database and segmentation by one hidden layer with 5 nodes.

Type of database and segmentation used	Percentage rate of testing confusion matrix (%)
Drive-Matched filter	73.76
Drions-Matched filter	53.34
HRF-Matched filter	53.32
Drive-Hough Transform	56.64
Drions-Hough Transform	43.32
HRF-Hough Transform	30.00
Drive-Morphological Operation	50.00
Drions-Morphological Operation	46.68
HRF-Morphological Operation	36.66
Drive-Watershed	53.32
Drions-Watershed	43.34
HRF-Watershed	60.0

From Table-5, we can see that the highest percentage rate is the recognition using Matched filter with Drive database. This means that Matched filter and Drive database can give accurate result in order to recognize the retinal images.

**2. Hidden layer = 10 nodes****Table-6.** Overall percentage rate of testing confusion matrix in each database and segmentation by one hidden layer with 10 nodes.

Type of database and segmentation used	Percentage rate of testing confusion matrix (%)
Drive-Matched filter	46.66
Drions-Matched filter	46.66
HRF-Matched filter	63.64
Drive-Hough Transform	26.68
Drions-Hough Transform	43.34
HRF-Hough Transform	46.66
Drive-Morphological Operation	50.00
Drions-Morphological Operation	40.02
HRF-Morphological Operation	50.00
Drive-Watershed	33.34
Drions-Watershed	60.00
HRF-Watershed	60.00



From Table-5, we can see that the highest percentage rate of testing confusion matrix is 63.64% by using single hidden layer with 10 nodes. The database and segmentation used are HRF and Matched filter.

### 3. Hidden layer = 15 nodes

**Table-7.** Overall percentage rate of testing confusion matrix in each database and segmentation by one hidden layer with 15 nodes.

Type of database and segmentation used	Percentage rate of testing confusion matrix (%)
Drive-Matched filter	53.32
Drions-Matched filter	50.02
HRF-Matched filter	53.34
Drive-Hough Transform	30.00
Drions-Hough Transform	50.00
HRF-Hough Transform	49.98
Drive-Morphological Operation	46.66
Drions-Morphological Operation	56.66
HRF-Morphological Operation	29.98
Drive-Watershed	73.32
Drions-Watershed	30.00
HRF-Watershed	50.00

From Table-7, we can see that Drive database and watershed segmentation give the highest percentage rate of confusion matrix which is 73.32% by using single hidden layer with 15 nodes.

### DISCUSSIONS

Four automatic segmentation methods which are matched filter, Hough Transform, Morphological operation and watershed, have been used to segment retinal eye vessels. Three datasets which are Drive, Drions and HRF databases have been used. From Table-1, the FP rate of Drive database is lesser comparable to the other two datasets. This is due to the varying of methods in terms of the images' compression and acquisition of images. However, in general, Matched filter has shown effectiveness in segmenting retinal image blood vessels.

From Figure-14, Hough Transform segmentation failed using Drions and HRF datasets. Meanwhile Drive dataset has shown better results as shown in Figure-14 (a). Table-2 shows that none of the three datasets methods has reached a level of accuracy. The Morphological segmentation has shown better results comparable to Hough Transform. From Figure 16, it is clear that Drive datasets has performed better than Drions and HRF

datasets. Summing up, the results obtained in Table-3 show that Drive database F-measure is better comparable to the other two datasets.

From the three Tables 4, 5 and 6, we can conclude that based on the effectiveness of retinal blood vessel segmentation and the percentage rate of testing confusion matrix in recognition process, the Matched filter segmentation and Drive database give the best accuracy in automatic detection of blood vessels followed by HRF database segmentation using Matched filter.

### CONCLUSIONS

Summing up briefly, this article explains the segmentation of retinal images for different potential applications of automatic diabetic diagnosis. We have used four different methods of segmenting retinal images which are Matched filter, Hough transform, Morphological operations and Watershed. In order to have better results, three different types of retinal images database which are DRIVE database, Drions database and HRF database have been tested. To create a database, 20 images included in training set and 20 images in test set. So, totally set of 40 images used for derived data set. Meanwhile Drions databases have a set of 110 images and 2 ground truths for each one. Lastly, there are three set of images in HRF database which each set have 15 images consist of healthy, diabetic retinopathy and glaucoma, respectively.

Different measures such as FP, TP, precision, recall and F-measure computed to evaluate the performance of each of the developed methods.

The obtained results using the aforementioned segmentation methods show that retinal images blood vessels can be automatically segmented and can be used for further diagnose. For recognition, we used ANN instead of other methods such as fuzzy logic and support vector machines. This is because ANN can give better accuracy in terms of recognizing the diabetic cells. The results obtained using Matched filter and Drive database have shown that using retinal images blood vessels segmentation can be a promising technique for diabetic retinopathy diagnose.

### REFERENCES

- [1] Al-Rawi, Mohammed, Munib Qutaishat, and Mohammed Arrar. 2007. "An improved Matched filter for blood vessel detection of digital retinal images." *Computers in Biology and Medicine*. 37.2, pp. 262-267.
- [2] Riveron E. F. and Guimeras N. G. 2006. Extraction of blood vessels in ophthalmic color images of human retinas, *Lecture Notes in Computer Science*, 4225: 118-126.





- [3] U.M Akram and A.S Khan. 2012. "Automated Detection of Dark and Bright Lesions in Retinal Images for Early Detection of Diabetic Retinopathy". Journal of Medical Systems, Volume 36, Issue 5.
- [4] Odstrcilik, J., Kolar, R., Budai, A., Horneegger, J., Jan, J., Gazarek, J., Kubena, T., Cernosek, P., Svoboda, O. and Angelopoulou, E. 2013. Retinal vessel segmentation by improved matched filtering: evaluation on a new high-resolution fundus image database, pp. 373-383.
- [5] Chaudhuri, S., Chatterjee, S., Katz, N., Nelson, M., Goldbaum, M. 1989. Detection of retinal blood vessels in retinal images using two-dimensional Matched filters. IEEE Trans. Med. Imag.8, pp. 263-369.
- [6] Patton, N., Aslam, T. M., Mac Gillivray, T., Deary, I. J., Dhillon, B., Eikelboom, R. H. and Constable, I. J. 2006. Retinal image analysis: concepts, applications and potential. Progress in retinal and eye research, 25(1), 99-127.
- [7] Hunter, A.,Lowell, J., Steel, D., Basu, A.,Ryder, R. 2002. Non-linear filtering for vascular segmentation and detection of venous beading. University of Durham.
- [8] Gonzalez, R., Woods, R. 2010. Digital Image Processing. 3<sup>rd</sup> ed. Pearson: Prentice Hall.
- [9] Rotaru, F., Bejinariu, S. I., Nita, C. D., Luca, R. and Lazar, C. 2014. Optic Disc Identification Methods for Retinal Images. Computer Science, 22(2), 65.
- [10] Sasaki, Y. 2007. The truth of the F-measure. In S. o. C. Science (Ed.): University of Manchester.